Cellular/Molecular

NMDA Receptor Surface Trafficking and Synaptic Subunit Composition Are Developmentally Regulated by the Extracellular Matrix Protein Reelin

Laurent Groc,[2] Daniel Choquet,[2] F. Anne Stephenson,[3] Danièle Verrier,[1] Olivier J. Manzoni,[1] and Pascale Chavis[1]

[1]Inserm, Unité 862, Equipe Physiopathologie de la Plasticité Synaptique, 33077 Bordeaux Cedex, France, [2]Physiologie Cellulaire de la Synapse, Centre National de la Recherche Scientifique, Unité Mixte de Recherche 5091, 33077 Bordeaux, France, and [3]School of Pharmacy, University of London, London WC1N 1AX, United Kingdom

During postnatal development, changes in the subunit composition of glutamate receptors of the NMDA subtype (NMDARs) are key to the refinement of excitatory synapses. Hypotheses for maturation of synaptic NMDARs include regulation of their expression levels, membrane targeting, and surface movements. In addition, several members of extracellular matrix (ECM) proteins such as Reelin are involved in synaptic plasticity. However, it is not known whether and how ECM proteins regulate synaptic NMDAR maturation. To probe the participation of NMDARs to synaptic currents and NMDARs surface dynamics, we used electrophysiological recordings and single-particle tracking in cultured hippocampal neurons. Our results show that, during maturation, Reelin orchestrates the regulation of subunit composition of synaptic NMDARs and controls the surface mobility of NR2B subunits. During postnatal maturation, we observed a marked decrease of NR1/NR2B receptor participation to NMDAR-mediated synaptic currents concomitant with the accumulation of Reelin at active synapses. Blockade of the function of Reelin prevented the maturation-dependent reduction in NR1/NR2B-mediated synaptic currents. The reduction of NR1/NR2B receptors was not inhibited by blocking synaptic activity but required β1-containing integrin receptors. Single-particle tracking showed that inhibition of Reelin decreased the surface mobility of native NR2B-containing NMDARs, whereas their synaptic dwell time increased. Conversely, recombinant Reelin dramatically reduced NR2B-mediated synaptic currents and the time spent by NR2B subunits within synapses. Our data reveal a new mode of control of synaptic NMDAR assembly at postnatal hippocampal synapses and an unprecedented role of ECM proteins in regulating glutamate receptor surface diffusion.

Key words: **NMDA receptor; Reelin; surface mobility; development; integrins; hippocampus**

Introduction

During postnatal development of the CNS, the dynamic maturation of synaptic contacts participates in the refinement of immature neuronal networks. Often associated with adult synaptic plasticity, the maturation of glutamatergic synapses involves recruitment or stabilization of ionotropic glutamate receptors (Garner et al., 2002; Groc et al., 2006a). The NMDA receptors (NMDARs) are heteromeric ligand-gated ion channels composed of NR1 subunits in combination with NR2 (NR2A–NR2D) or NR3 subunits. The expression pattern of the different NR2 subunits is regionally and developmentally regulated. At most excitatory synapses, NR2B-containing NMDARs (2B–NMDARs) are abundant at early stages and gradually replaced or supplemented by NR2A-containing NMDARs (2A–NMDARs) (Monyer et al., 1994; Sheng et al., 1994; Shi et al., 1997; Kew et al., 1998; Li et al., 1998; Stocca and Vicini, 1998; Tovar and Westbrook, 1999; Thomas et al., 2006). Importantly, the functional properties of NMDARs depend on their subunit composition, and such subunit heterogeneity of synaptic NMDARs is thought to play a crucial role in synaptic maturation and plasticity processes (van Zundert et al., 2004; Perez-Otano and Ehlers, 2005). In addition to changes in insertion and recycling of NMDARs subunits (Roche et al., 2001; Wenthold et al., 2003; Lavezzari et al., 2004), lateral mobility of glutamate receptors has emerged as a process to modulate not only the number of synaptic receptors (Borgdorff and Choquet, 2002; Tovar and Westbrook, 2002; Ashby et al., 2004; Groc et al., 2004; Adesnik et al., 2005) but also the subunit composition of NMDARs (Groc et al., 2006b). In hippocampal neurons, NMDARs exchange rapidly between the

Received April 19, 2007; revised Aug. 1, 2007; accepted Aug. 2, 2007.

This work was supported by Inserm (O.J.M., P.C.), Région Aquitaine (P.C., O.J.M., L.G., D.C.), Agence Nationale de la Recherche Grant 06-037-01 "Neurosciences, Neurologie et Psychiatrie" (P.C.), Centre National de la Recherche Scientifique (L.G., D.C.), Ministère de la Recherche (L.G., D.C.), Fondation pour la Recherche Médicale (L.G., D.C., P.C., O.J.M.), Association Française contre les Myopathies (L.G., D.C.), Human Frontier Science Program (L.G., D.C.), and European Community Grants QLG3-CT-2001-02089 and CT-2005-005320 (L.G., D.C.). We thank Dr. K. Nakajima (Keio University, Tokyo, Japan) for the CR-50 antibody, Dr. E. J. Weeber (Vanderbilt University, Nashville, TN) for recombinant Reelin, Dr. T. E. Willnow (Max Delbrück Center for Molecular Medicine, Berlin, Germany) for the expression construct of GST-tagged RAP, and Dr. J. Blahos (Prague, Czech Republic) for the expression of GST–RAP. We thank Dr. G. Westbrook for helpful discussions.

Correspondence should be addressed to either of the following: Pascale Chavis, Inserm, Unité 862, 146 rue Leo Saignat, 33077 Bordeaux Cedex, France, E-mail: chavis@bordeaux.inserm.fr; or Laurent Groc, Centre National de la Recherche Scientifique, Unité Mixte de Recherche 5091, 33077 Bordeaux Cedex, France, E-mail: laurent.groc@u-bordeaux2.fr.

DOI:10.1523/JNEUROSCI.1772-07.2007

 0270-6474/07/2710165-11$15.00/0

extrasynaptic and synaptic membranes (Tovar and Westbrook, 2002), and developmental changes in surface trafficking of different NR2 subunits correlate with changes in synaptic NMDAR composition (Groc et al., 2006b). However, the molecular processes that govern surface trafficking of NMDAR subunits during synaptic maturation remain unknown.

Several members of the extracellular matrix (ECM) proteins and cell adhesion molecules have been proposed to orchestrate the subunit composition of NMDARs and therefore their synaptic functions (Dityatev and Schachner, 2003). As we reported previously, cell adhesion molecules of the integrin family coordinate the maturation of the presynaptic and postsynaptic compartments in the hippocampus (Chavis and Westbrook, 2001). The ECM protein Reelin, known for its importance in the development of laminar structures (D'Arcangelo and Curran, 1998), has been proposed to also participate in postnatal and adult neuronal functions (Tissir and Goffinet, 2003). Reelin is a large secreted glycoprotein that acts as a signaling molecule by binding to different classes of receptors (D'Arcangelo et al., 1999; Dulabon et al., 2000). Exogenous application of recombinant Reelin (rRln) has been reported to modulate glutamatergic synaptic plasticity in the hippocampus (Beffert et al., 2005; Qiu et al., 2006). Despite numerous studies aimed at elucidating the role of Reelin in the normal postnatal brain, the physiological role of endogenously secreted Reelin at glutamatergic hippocampal synapses remains poorly understood. In the present study, we found that Reelin controlled in a bidirectional manner the changes in the subunit composition of functional synaptic NMDARs during maturation. This effect involved receptors of the integrin family. Using single-nanoparticle tracking, we observed that the Reelin-dependent maturation of synaptic NMDARs was paralleled by changes of the surface mobility of NR2B-containing NMDARs, showing for the first time that lateral mobility of ionotropic glutamate receptors is regulated by ECM proteins.

Materials and Methods

Cell culture and reagents. Cell cultures were performed as described previously (Sinagra et al., 2005). Chronic treatments with rRln and the mock control 2.50–5.55 nM [produced as described previously (Sinagra et al., 2005)] were performed at 7 d *in vitro* (div). Chronic treatments with the following reagents were performed at 9.5 div: CR-50 antibody at 30–100 μg/ml, normal mouse IgG at 30–100 μg/ml (Jackson ImmunoResearch via Interchim, Montlucon, France) receptor-associated protein fused with glutathione *S*-transferase (GST-RAP) at 10–50 μg/ml, GST at 10–50 μg/ml, hamster anti-rat β1 monoclonal antibody at 50–100 μg/ml (BD Biosciences PharMingen, Le Pont de Claix, France), nonimmune hamster IgM at 50–100 μg/ml (BD Biosciences PharMingen), tetrodotoxin (TTX) (1 μM; Alomone Labs, Jerusalem, Israel), and Reelin antisense (RlnAS) and control mismatched (RlnM) at 10 μM (Eurogentec, Seraing, Belgium). The sequences of the Reelin phosphorothioate antisense and the corresponding mismatched oligonucleotide were as described previously [RlnAS, 5′-GCAATGTGCAGGGAAATG-3′; and RlnM, 5′-ACCTTGTGACCCATCTCT3′ (Sinagra et al., 2005)]. Acute treatments with rRln or mock were performed at 7 or 8 div for 1 to 20 min duration.

Animals. All experiments were conducted in strict compliance with European directives and French laws on animal experimentation (authorization number 3307016).

Data. Each set of experiments was performed on three to five different cultures. All data are presented as mean ± SEM or median ± 25–75% interquartile range (IQR).

Electrophysiology. Neurons were continuously perfused with Mg^{2+}-free extracellular solution containing the following (in mM): 160 NaCl, 2.4 KCl, 10 HEPES, 10 glucose, 0.02 glycine, and 1.5 $CaCl_2$, pH 7.3 (osmolarity, 325 mOsm/liter). Patch pipettes (2–4.5 MΩ) were filled with the following (in mM): 149 Cs-methanesulfonate, 1 EGTA, 10 HEPES, 4 $MgCl_2$, 10 glucose, and 2 Na_2ATP, pH 7.3 (osmolarity, 305–310 mOsm/liter). Data were acquired using an Axopatch 200 B and Clampex 8 (Molecular Devices via, DIPSI, Chatillon, France) acquisition software. Currents were filtered at 2 kHz and digitized at 5 kHz. Miniature EPSCs (mEPSCs) were recorded at −70 mV. Miniature NMDA–EPSCs were isolated in the presence of TTX (0.3 μM), bicuculline (10 μM; Tocris Biosciences via Fisher Bioblock, Illkirch, France), and CNQX (10 μM; Tocris Biosciences), then were recorded in the presence of 3 μM ifenprodil (Sigma, St. Quentin Fallavier, France), and finally were blocked with D-APV (25 μM; Tocris Bioscience) at the end of each experiment. Dual-component mEPSCs were collected in the absence of CNQX before and during ifenprodil application (3 μM).

mEPSC amplitude and interinterval time were analyzed with Axograph 4.0 (Molecular Devices via DIPSI) using a double-exponential template: $f(t) = \exp(-t/\text{rise}) + \exp(-t/\text{decay})$, where rise is 3 ms and decay is 10 ms for NMDA–mEPSCs, and rise is 0.5 ms and decay is 3 ms for AMPA–mEPSCs. The limit of detection was >5 pA. Statistics were assessed using ANOVA, followed, if significant ($p < 0.05$), by Tukey's multiple comparison test (Kyplot 2.0 β13). Kolmogorov–Smirnov (KS) tests were used for comparing the cumulative distributions of interevent intervals (Kyplot 2.0 β13). The decay times of NMDA–mEPSCs were fitted using one and two exponentials (Axograph 4.0; Molecular Devices), and the sum of squared errors for single-exponential fits was 2.3 times better than for a two-exponential fit.

Quantum dot tracking. Single particles [quantum dots (QDs)] were detected and tracked as described previously (Groc et al., 2006b). Briefly, QD 655 goat F(ab′)2 anti-rabbit IgG (0.1 μM; Ozyme, St. Quentin Fallavier, France) were incubated for 30 min with the polyclonal antibodies against NR2A or NR2B (1 μg). Synapses were labeled with Green Mitotracker (1 min, 1 nM at room temperature; Invitrogen, Carlsbad, CA). Then, neurons were incubated for 10 min at 37°C in culture medium with precoated QDs (final dilution 0.1 nM).

QD-labeled NR2 subunits were followed exclusively on randomly selected neuritic regions. Somata were not included for analysis. Signals were detected using a CCD camera (Cascade; Princeton Instruments, Trenton, NJ). Images of Mitotracker-labeled synapses were acquired with the filter set HQ500/20× for excitation (Chroma Technology, Brattleboro, VT) and HQ560/80M for emission (Chroma Technology). QDs were detected by using a xenon lamp (excitation filter 560RDF55 and emission filter 655WB20; Omega, Guyancourt, France), and images were obtained with an integration time of 50 ms, with up to 1200 consecutive frames. Recording sessions were acquired within 30 min after primary antibody incubation to minimize receptor endocytosis.

QD recording sessions were processed with the MetaMorph software (Universal Imaging, Downingtown, PA). The instantaneous diffusion coefficient, *D*, was calculated for each trajectory, from linear fits of the first four points of the mean square displacement (MSD) versus time function using $\text{MSD}(t) = \langle r^2 \rangle (t) = 4Dt$. Synaptic dwell time was calculated for exchanging receptors and defined as the mean time spent within the synaptic area. The two-dimensional trajectories of single molecules in the plane of focus were constructed by correlation analysis between consecutive images using a Vogel algorithm. Statistical significance was assessed with Mann–Whitney *U* tests (diffusion coefficient comparison) and Student's *t* test (dwell-time comparison).

Immunoblotting. Western blotting of Reelin and processing of dishes were performed as described previously (Sinagra et al., 2005). Samples of 50 μg of homogenate proteins run through the same 6% SDS-PAGE were subjected at the same time to protein quantification with the BCA protein assay kit (Pierce, Rockford, IL; Fisher Bioblock). Secreted Reelin measured in cultured cell media and intracellular Reelin isolated from scraped neurons were collected from the same dishes. Chronic treatments with TTX and processing of culture dishes were performed after a double-blind protocol to avoid any bias.

Immunoblots chemiluminescence was acquired with ChemiGenius 2 (SynGene via Ozyme), and band densities were quantified with GeneTools (SynGene via Ozyme). For each gel, the density measurements were added over the three bands obtained for the three isoforms and normalized to total Reelin in untreated conditions.

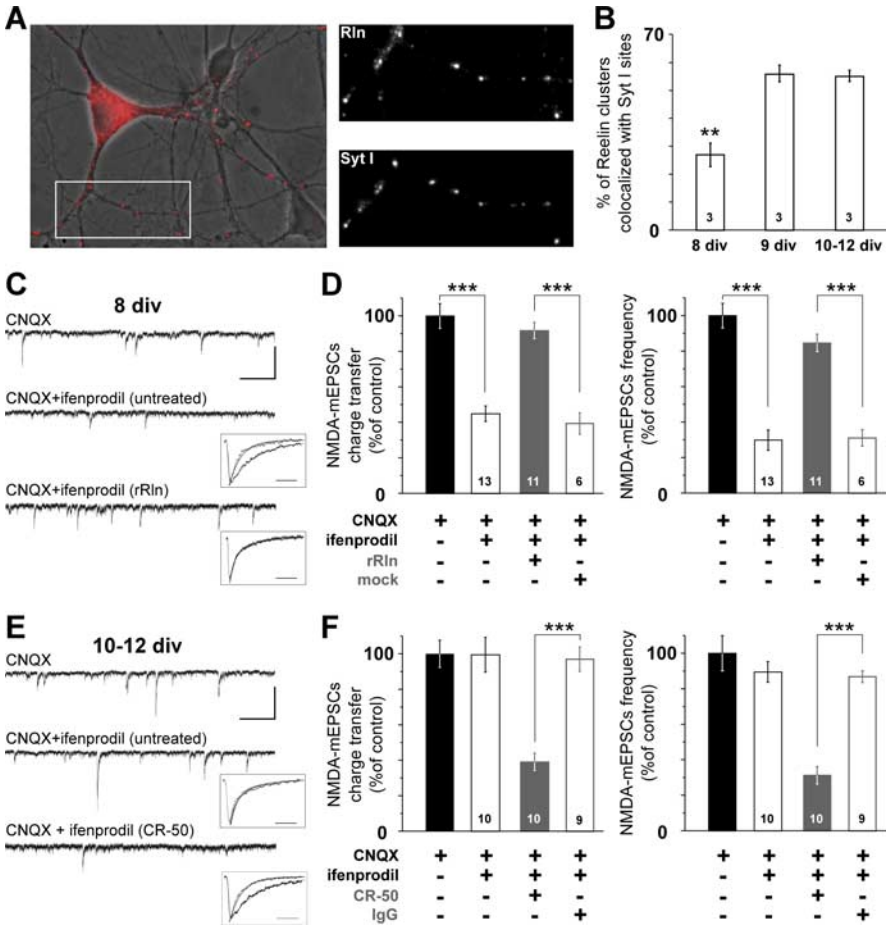

Figure 1. Reelin controls the subunit composition of synaptic NMDAR during maturation. ***A***, Left, Overlaid pseudocolor image of Reelin labeling (red) and the corresponding differential interference contrast image in a 12 div culture showing a marked punctuate labeling on neurites. Right panels show higher-magnification views of neurites labeled with anti-Reelin and anti-SytI antibodies of the area boxed at the left. ***B***, Synaptic enrichment of Reelin during maturation. Percentage ± SEM of Reelin-positive puncta colocalized with Syt I immunoreactivity ($n = 3$ cultures; $F_{(2,6)} = 27.7$; $^{**}p < 0.01$). ***C***, Representative 15 s recordings of NMDA–mEPSCs with CNQX (top) or CNQX plus ifenprodil in a untreated neuron (middle) or rRln-treated neuron (bottom; calibration: 50 pA, 2 s). Insets, Averaged and scaled NMDA–mEPSCs before (black) and after ifenprodil application (gray) taken from the illustrated cells. The decay phases were best fitted with a monoexponential (solid traces; calibration, 50 ms) (see Materials and Methods). ***D***, Effect of ifenprodil on NMDA–mEPSC charge transfer and frequency in untreated conditions (open black) and after rRln treatment (gray) or the mock control (open gray). Values obtained with CNQX were expressed as a percentage of the mean CNQX value. Black bars represent the percentage average ± SEM obtained in untreated neurons in CNQX (i.e., control). The effect of ifenprodil is expressed as percentage of CNQX ± SEM obtained in each condition. ANOVA revealed significant differences between the various conditions for charge transfer ($F_{(3,39)} = 27.4$) and frequency ($F_{(3,39)} = 44.9$). $^{***}p < 0.001$. The number of neurons recorded in each condition is indicated. ***E***, Representative 15 s recordings of NMDA–mEPSCs in the presence of CNQX (top) or CNQX and ifenprodil in either untreated neuron (middle) or neuron treated with CR-50 (bottom; calibration: 50 pA, 2 s). Inset, Same legend as ***C***. ***F***, Same legend as ***D*** but instead neurons were chronically treated with CR-50 (gray) or a control IgG (open gray). ANOVA revealed significant differences between untreated, CR-50, and mock conditions for charge transfer ($F_{(3,35)} = 28.9$) and frequency ($F_{(3,35)} = 21.3$). $^{***}p < 0.001$.

Immunostainings. Reelin immunostaining and live uptake of anti-SytI antibodies (Calbiochem via VWR International, West Chester, PA) were performed as described previously (Chavis et al., 1998). Surface NR2A and NR2B subunits were stained by incubating live neurons with 10 μg of affinity-purified polyclonal antibodies against the N-terminal domain of NR2A or NR2B (Groc et al., 2006b). The surface fluorescence was quantified as described previously (Groc et al., 2006b) using the average intensity and pixel area on the dendritic field. Somata were excluded from analysis. On randomly selected dendritic segments, clusters were isolated by applying a constant threshold on images, and their integrated intensity was measured. All analysis was performed with MetaMorph software (Universal Imaging). Statistical significance was assessed with Student's *t* test.

Results

Reelin is sufficient to induce the maturation of synaptic NMDARs

In hippocampal neurons *in vitro*, Reelin immunoreactivity probed with the well characterized G10 antibody (Sinagra et al., 2005; Ramos-Moreno et al., 2006) displayed a neuritic punctuated pattern suggestive of synaptic labeling (Fig. 1*A*). Active synapses were tagged in living neurons using the dynamic uptake of an antibody targeted against the luminal epitope of the vesicular protein synaptotagmin I (Syt I) (Chavis et al., 1998). Colabeling Reelin and active synapses revealed that, between 8 and 9–12 div, a time critical for maturational processes, Reelin accumulates at developing synapses (Fig. 1*A*,*B*).

These results prompted us to examine whether Reelin governed NMDAR subunit composition during glutamatergic synaptic maturation. Thus, to evaluate the developmental profile of synaptic NR1/NR2B during maturation of hippocampal neurons *in vitro*, the effect of the noncompetitive NR2B-selective antagonist ifenprodil (Williams, 1993) was measured on NMDA–mEPSCs. We used the highest concentration of ifenprodil (3 μM) that does not affect 2A–NMDARs (Williams, 1993; Tovar and Westbrook, 1999). At 8 div, ifenprodil decreased NMDA–mEPSC charge transfer to 44.9 ± 4.4% of the control value (Fig. 1*C*,*D*). The deactivation kinetics of NMDA–mEPSCs were markedly faster in the presence of ifenprodil (Table 1; Fig. 1*C*, inset), consistent with the blockade of NR1/NR2B receptors (Kirson and Yaari, 1996; Flint et al., 1997; Kew et al., 1998; Tovar and Westbrook, 1999). Ifenprodil also reduced NMDA–mEPSC frequency (29.8 ± 5.7% of control value) (Fig. 1*D*) and caused a significant shift in the distribution of NMDA–mEPSCs interevent intervals ($p < 1.10^{-10}$, KS test) (supplemental Fig. 1*A*, available at www.jneurosci.org as supplemental material). Because neither the frequency nor the amplitude of AMPA glutamate receptor (AMPAR)-mediated miniature events were modified by ifenprodil (Fig. 2*A*,*B*), we concluded that ifenprodil acted on postsynaptic NR1/NR2B receptors. To mimic the extracellular environment observed at later maturational stages, i.e., increased extracellular Reelin content (Sinagra et al., 2005), we complemented immature hippocampal neurons with rRln at 7 div (see Materials and Methods). The 24 h treatment with rRln totally suppressed all the effects of ifenprodil. The NMDA–mEPSCs charge transfer and frequency in the presence of ifenprodil represented 84.6 ± 4.9 and 91.8 ± 4.6% of CNQX conditions, respectively (Fig. 1*D*), values significantly different from untreated and mock-treated conditions. In contrast to untreated or mock-

Table 1. Deactivation kinetics of NMDA–mEPSCs at different ages of *in vitro* maturation and after various chronic treatments

Age (div)	Treatment	τ_{CNQX} (ms)	$\tau_{CNQX + ifenprodil}$ (ms)	p	n
8		95.2 ± 15.2	25.0 ± 7.8	7.10^{-8}	13
10–12		35.9 ± 4.1	39.6 ± 5.2	0.08	10
8	rRln	30.2 ± 5.9	32.1 ± 6.3	0.15	11
8	Mock	93.0 ± 17.2	25.2 ± 6.6	3.10^{-4}	6
10–12	CR-50	84.0 ± 17.5	31.4 ± 1.8	4.10^{-4}	10
10–12	IgG	33.7 ± 4.6	36.1 ± 5.6	0.32	9
10–12	Anti-β1	96.1 ± 14.1	27.3 ± 8.5	4.10^{-4}	7
10–12	IgM	30.1 ± 5.3	33.4 ± 4.7	0.25	8

Within each condition, the average decay time constants were estimated (see Materials and Methods) before (τ_{CNQX}) and during ($\tau_{CNQX + ifenprodil}$) ifenprodil application. Statistical differences were assessed before and after ifenprodil application with Student's *t* test.

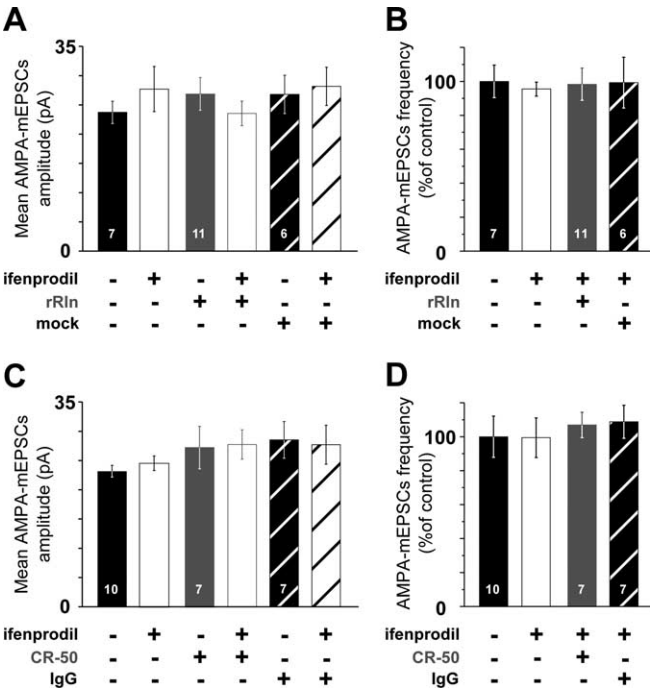

Figure 2. Recombinant Reelin and CR-50 do not affect AMPA–mEPSC amplitude or frequency. ***A***, AMPA–mEPSC mean amplitude at 8 div before ifenprodil application and with ifenprodil, in untreated neurons (black and open black; $n = 7$ neurons, 4 cultures), in rRln-treated neurons (gray and open gray; $n = 11$ neurons, 3 cultures), and in mock-treated neurons (hatched white and black; $n = 6$ neurons, 3 cultures). ANOVA did not reveal significant differences between various groups ($p = 0.09$). ***B***, Frequencies of AMPA–mEPSCs before (black) and in the presence of ifenprodil (open black) in 8 div untreated neurons, in rRln-treated (gray), or mock-treated (hatched white) neurons were not significantly different ($p = 0.3$, ANOVA). Values in the presence of ifenprodil are expressed as the percentage ± SEM of the mean control value obtained before ifenprodil application. ***C***, Same legend as ***A*** in 10–12 div neurons untreated ($n = 10$ neurons, 5 cultures), treated with CR-50 (gray and open gray; $n = 7$ neurons, 3 cultures), or the control IgG (hatched white and black; $n = 7$ neurons, 3 cultures). ANOVA did not reveal significant differences between various groups ($p = 0.12$). ***D***, AMPA–mEPSC frequencies in 10–12 div neurons were not significantly different between untreated before ifenprodil (black), untreated with ifenprodil (open black; $n = 10$ neurons, 5 cultures), CR-50 (gray; $n = 7$ neurons, 3 cultures), and IgG (hatched white; $n = 7$ neurons, 3 cultures; $p = 0.67$, ANOVA).

treated neurons of the same age, the interevent intervals distribution of NMDA–mEPSCs were not altered in the presence of ifenprodil ($p = 0.52$, KS test) (supplemental Fig. 1*C*, available at www.jneurosci.org as supplemental material). The rRln treatment did not change the frequency of the total NMDA–mEPSC population (before ifenprodil application) compared with untreated and mock conditions [$p = 0.99$ ANOVA and compare distributions in supplemental Fig. 1*A*,*C* (available at www.jneurosci.org as supplemental material), $p = 0.42$, KS test]. The loss of the ifenprodil sensitivity in rRln-treated neurons was also observed on the deactivation kinetics. The average decay times were not significantly changed by ifenprodil (Table 1, Fig. 1*C*) and were significantly shorter before ifenprodil application compared with untreated conditions ($p = 2.9.10^{-5}$, *t* test). These results suggest that Reelin controls the maturation of synaptic NMDARs.

The function of Reelin is necessary for normal maturation of synaptic NMDARs *in vitro*

In 10–12 div neurons, ifenprodil had no effects on NMDA–mEPSC charge transfer and frequency (99.4 ± 9.8 and 89.5 ± 5.8% of control, respectively; $p > 0.05$) (Fig. 1*E*,*F*) or interevent intervals distribution ($p = 0.49$, KS test) (supplemental Fig. 1*B*, available at www.jneurosci.org as supplemental material). The maturational loss of ifenprodil sensitivity was accompanied by a speeding of the NMDA–mEPSC decay (Table 1; Fig. 1*E*, inset) compared with 8 div untreated conditions ($p = 0.0002$, *t* test). Neither the amplitude nor the frequency of AMPA–mEPSCs was changed by ifenprodil (Fig. 2*C*,*D*). Thus, hippocampal mature synapses are devoid of functional highly ifenprodil-sensitive NR1/NR2B receptors and display NMDA–mEPSCs with faster kinetics, in agreement with a change in the subunit composition of NMDARs to NR1/NR2A and/or NR1/NR2A/NR2B (Sheng et al., 1994; Kirson and Yaari, 1996; Flint et al., 1997; Li et al., 1998; Tovar and Westbrook, 1999; Thomas et al., 2006).

Strikingly, values obtained after treatment with rRln were not statistically different from that of 10–12 div untreated neurons, showing that addition of rRln accelerated synaptic maturation. Having shown that increasing Reelin levels accelerated synaptic maturation of NMDARs, we next tested whether the function of Reelin was necessary for the maturational process that governs NMDAR subunit composition at synapses. We chronically treated 10–12 div neurons (see Materials and Methods) with the CR-50 antibody that has function-interfering activity of Reelin both *in vivo* and *in vitro* (Ogawa et al., 1995; Miyata et al., 1997; Nakajima et al., 1997). In 10–12 div neurons treated with CR-50, ifenprodil drastically reduced the charge transfer and the frequency of NMDA–mEPSCs to 39.1 ± 4.9 and 31.2 ± 4.9% of control values, respectively (Fig. 1*E*,*F*), as well as the interevent interval distribution ($p < 1.10^{-10}$, KS test) (supplemental Fig. 1*D*, available at www.jneurosci.org as supplemental material). The control IgG had no effect (Fig. 1*F*, Table 1). The deactivation kinetics were faster after ifenprodil application in CR-50-treated neurons (Table 1, Fig. 1*E*) and slower before ifenprodil application compared with untreated 10–12 div ($p = 3.10^{-5}$, *t* test). The interevent intervals distribution of the total NMDA–mEPSCs population, which combines both ifenprodil- sensitive and

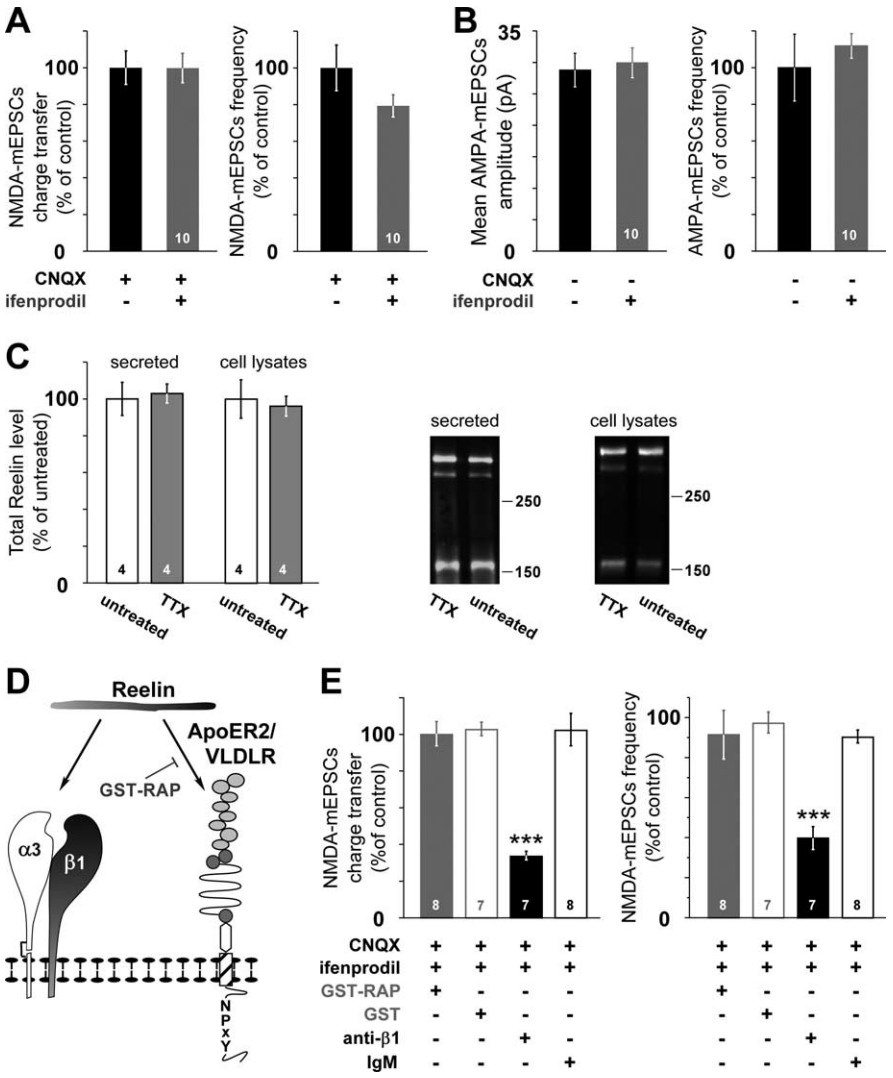

Figure 3. The change in the subunit composition of synaptic NMDAR is independent of *in vitro* activity but involves β1-class integrins. ***A***, NMDA–mEPSC charge transfer and frequency in 10–12 div neurons chronically treated with TTX. Values are expressed as in Figure 1*D*. ***B***, AMPA–mEPSC amplitude and frequency in 10–12 div neurons chronically treated with TTX ($n = 10$ neurons, 4 cultures). ***C***, Western blot analysis of Reelin present in the culture medium (secreted) or in cell lysates from untreated and TTX-treated 10 div hippocampal cultures. Right, Densitometry measurements of secreted or intracellular Reelin in TTX-treated dishes (gray) are expressed as the percentage ± SEM of 10 div untreated (open bar; $n = 4$ cultures). Values obtained in untreated cultures were expressed as a percentage of the mean untreated value. Right, A full-length Reelin (400 kDa) and the fragments produced by cleavage (320, 180 kDa) are disclosed by the G10 antibody. ***D***, Schematic representation of the different inhibitors used to target the receptors of Reelin. ***E***, Chronic treatment of 10–12 div neurons with the anti-β1 function-blocking antibody (black) induced significant changes in the ifenprodil sensitivity of NMDA–mEPSC charge transfer ($F_{(3,26)} = 26.17$) and frequency ($F_{(3,26)} = 20.3$) compared with treatments with the control IgM (open black), GST–RAP (gray), or GST (open gray); $^{***}p < 0.001$.

-insensitive NMDA responses, was not altered after chronic treatment with CR-50 (compare black circles in supplemental Fig. 1*B*,*D*, available at www.jneurosci.org as supplemental material) ($p = 0.19$, KS test), suggesting that the recovery of the ifenprodil sensitivity after chronic treatment resulted from the presence of postsynaptic NR1/NR2B NMDARs. Blocking Reelin biosynthesis with antisense oligonucleotides [RlnAS (Sinagra et al., 2005)] mimicked the effect of CR-50 (frequency and charge transfer in the presence of ifenprodil were 28.5 ± 5.4 and 37.2 ± 1.8% of control respectively; $n = 8$ neurons, 3 cultures) compared with age-matched neurons treated with the mismatched oligonucleotide (frequency and charge transfer in the presence of ifenprodil were 86.9 ± 3.5 and 106.4 ± 7.8% of control, respectively; $n = 6$ neurons, 3 cultures). Finally, chronic treatment with rRln or CR-50 did not affect AMPA–mEPSCs compared with age-matched mock- and IgG-treated conditions showing that Reelin specifically controlled NMDARs (Fig. 2).

Together, the results show that neutralizing the function of Reelin prevented the loss of functional synaptic NR1/NR2B receptors normally observed during this maturational period and that Reelin controls the presence of NR1/NR2B in the synaptic compartment.

Reelin levels and the subunit composition of synaptic NMDARs are not controlled by activity *in vitro*

Because neuronal activity regulates different aspects of NMDAR functions (Perez-Otano and Ehlers, 2005), we investigated whether changes in the subunit composition of synaptic NMDARs were also controlled by neuronal activity. Chronic arrest of neuronal activity with TTX did not modify either the ifenprodil sensitivity of 10–12 div NMDA–mEPSCs (Fig. 3*A*) ($p = 0.61$ and $p = 0.08$, ANOVA) or the frequency and amplitude of AMPA–mEPSCs (Fig. 3*B*) ($p = 0.45$ and $p = 0.51$, ANOVA). The fact that Reelin was found localized in secretory vesicles and axons *in vivo* (Derer et al., 2001; Martinez-Cerdeno et al., 2003; Ramos-Moreno et al., 2006) as well as at active synapses *in vitro* (Fig. 1*A*,*B*) prompted us to examine whether Reelin levels were controlled by neuronal activity. Chronic treatment with TTX did not affect the levels of secreted or intracellular Reelin in 10 div cultures (Fig. 3*C*). These results indicate that neuronal activity *in vitro* does not control the proportion of functional synaptic 2B–NMDAR nor Reelin secretion in 10–12 div cultures.

Role of Reelin receptors in the subunit composition change of synaptic NMDARs

Secreted Reelin binds apolipoprotein E receptors 2 (ApoER2), the very-low-density lipoprotein receptor (VLDLR) (D'Arcangelo et al., 1999), and the $\alpha 3\beta 1$ of the integrin family (Dulabon et al., 2000) (Fig. 3*D*). Cultures were chronically treated with RAP fused with GST. RAP is a molecular chaperone for the low-density lipoprotein receptor family, and it is widely used as a functional lipoprotein receptor antagonist (Herz et al., 1991) that prevents the binding of Reelin to ApoER2 and VLDLR, thus disrupting the physiological functions of Reelin (Hiesberger et al., 1999; Niu et al., 2004; Sinagra et al., 2005; Qiu et al., 2006) (Fig. 3*D*). Neither chronic treatment with GST–RAP nor the control GST restored the ifenprodil sensitivity in 10–12 div neurons (Fig. 3*E*), ruling out the involvement of the ApoER2/VLDLR receptors. On the same cells, we verified the efficacy of GST–RAP on whole-cell NMDA-evoked currents, a treatment we showed previously to efficiently block the somatic effects of Reelin (Sin-

agra et al., 2005). To test the involvement of $\alpha 3\beta 1$, we blocked $\beta 1$-class integrins with a function-blocking antibody against the $\beta 1$ subunit of the integrins. Chronic treatment with this antibody mimicked the effect of impairing Reelin functions (Fig. 3*E*, Table 1). NMDA–mEPSC charge transfer and frequency in the presence of ifenprodil represented 34.0 ± 2.3 and 39.8 ± 5.7% of control in anti-$\beta 1$-treated neurons and 102.6 ± 8.9 and 90.5 ± 3.3% in IgM-treated neurons, respectively. None of these treatments affected the frequency or the amplitude of AMPA–mEPSCs (data not shown), showing specificity for NMDARs. Altogether, these results suggest that the nonclassical Reelin receptor $\alpha 3\beta 1$ is involved in the subunit composition changes of synaptic NMDARs.

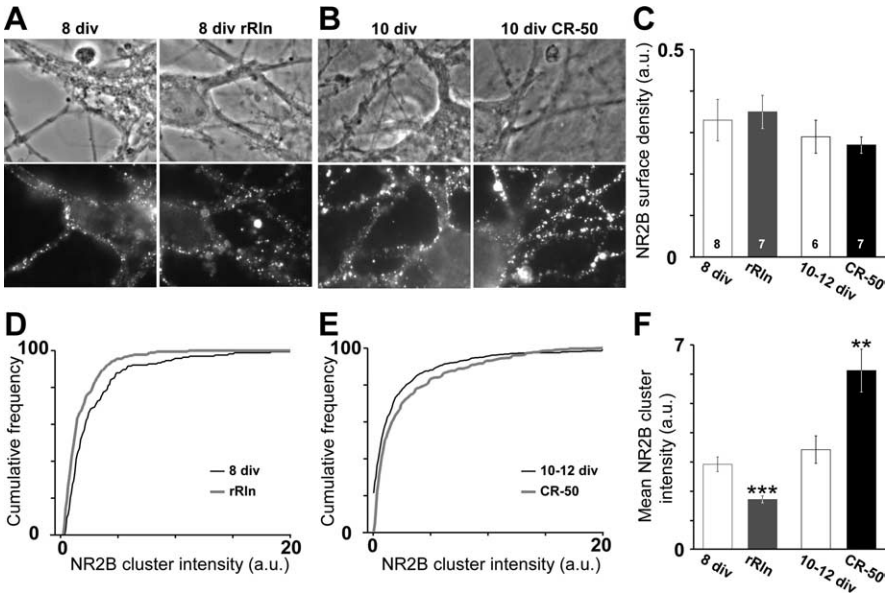

Figure 4. Reelin controls NR2B surface cluster intensity but not total surface density. ***A***, ***B***, Representative images of the surface NR2B staining and the corresponding differential interference contrast field in 8 div cultures (***A***) treated either with the control mock (left) or rRln (right) and in 10 div cultures (***B***) treated either with the control IgG (left) or CR-50 (right). ***C***, The NR2B surface expression was not modified by rRln or CR-50 treatments. Data are expressed as mean intensity/area units (a.u.) ± SEM. ***D***, ***E***, Cumulative distributions of the intensities of neuritic NR2B clusters in 8 div neurons (***D***) treated either with the control mock (black line) or rRln (gray line) and in 10–12 div neurons (***E***) chronically treated with the control IgG (black) or CR-50 (gray). ***F***, The average ± SEM intensity of NR2B clusters was significantly decreased by chronic rRln treatment (gray; $n = 181$) compared with mock control (open gray; $n = 166$; $^{***}p < 0.001$), whereas chronic treatment with CR-50 (black; $n = 587$) significantly increased the mean NR2B clusters intensity compared with control IgG (open black; $n = 524$; $^{**}p < 0.01$).

Reelin regulates surface distribution of native NR2B but not NR2A subunits

We next explored the molecular mechanisms mobilized by Reelin to control the synaptic content of 2B–NMDARs. Previous experiments were not consistent with changes in the synthesis levels of NR2B as the principal mode for Reelin to regulate the presence of 2B–NMDAR (Sinagra et al., 2005). Knowing that changes in glutamate receptor recycling correlate with modifications in surface receptor content (Ashby et al., 2004), we investigated whether Reelin controlled the overall content of surface 2B–NMDAR using antibodies directed against specific extracellular epitopes of the NR2A and NR2B subunits (Groc et al., 2006b). Surface immunostainings of NR2A and NR2B subunits in control conditions were qualitatively different as described previously (Groc et al., 2006b). NR2B showed both diffuse and punctate staining (Fig. 4*A*,*B*), whereas NR2A displayed a stronger punctate staining (supplemental Fig. 2, available at www.jneurosci.org as supplemental material). We observed that NR2B surface expression did not significantly vary during maturation (Fig. 4*A*,*B*), whereas, in agreement with our previous report (Groc et al., 2006b), a significant increase in the surface expression of native NR2A was observed between 8 and 10–12 div ($p = 0.045$) (supplemental Fig. 2*C*, available at www.jneurosci.org as supplemental material). Importantly, NR2B surface expression was not significantly affected by addition of rRln or blockade of Reelin function with CR-50 (Fig. 4*C*). Similarly, NR2A surface expression was not significantly affected by rRln or CR-50 (supplemental Fig. 2, available at www.jneurosci.org as supplemental material). These results indicate that changes in the total content of surface 2B–NMDAR or 2A–NMDAR could not account for the control of synaptic NMDAR composition by Reelin.

We next examined whether rRln or CR-50 induced changes in the surface distribution of 2B–NMDARs. We measured the integrated intensities of surface 2B–NMDAR clusters (Fig. 4) (supplemental Fig. 3, available at www.jneurosci.org as supplemental material) and found that chronic treatment with rRln significantly decreased the fluorescence intensity of 2B–NMDAR clusters in 8 div neurons (Fig. 4*D*,*F*). On the contrary, chronic blockade of the function of Reelin in 10–12 div neurons increased the fluorescence intensity of 2B–NMDAR clusters (Fig. 4*E*,*F*). None of these treatments affected the cluster area (data not shown). Interestingly, chronic treatment with CR-50 did not affect the fluorescence intensity of 2A-NMDAR clusters (control, 3.4 ± 0.3 arbitrary units, $n = 143$ clusters; CR-50, 3.5 ± 0.3 arbitrary units, $n = 159$; $p = 0.72$). These results indicate that the Reelin-dependent control of synaptic NMDAR subunit composition is paralleled by changes in the surface distribution of 2B–NMDARs.

Reelin controls the surface diffusion of native NR2B subunits

NMDARs diffuse within the plasma membrane of neurons and exchange rapidly between the extrasynaptic and synaptic compartments (Tovar and Westbrook, 2002; Groc et al., 2004, 2006b). Thus, we tested the challenging hypothesis that Reelin controls NMDAR surface distribution by affecting their surface mobility. We used the single-nanoparticle approach to track single QD coupled to antibodies directed against the extracellular epitope of NR2B (QD–NR2B) (Fig. 5) (supplemental Fig. 4, available at www.jneurosci.org as supplemental material). In control conditions, QD–NR2B displayed a heterogeneous behavior, including highly mobile and immobile trajectories. The dwell time of QD–NR2B in synaptic compartments decreased during maturation [1.1 ± 0.2 s in 8 div neurons, $n = 132$; 0.24 ± 0.02 s in 10 div neurons, $n = 206$; $p = 0.00028$ (Groc et al., 2006b)]. As illustrated by the QD–NR2B summed trajectories, chronic treatment with rRln strongly increased the explored area compared with age-matched mock conditions in 8 div neurons (Fig. 5*A*). When examined within synapses (see Materials and Methods), the surface mobility of 2B–NMDARs was significantly increased in rRln-treated neurons when compared with age-matched controls (Fig. 5*C*, left). This effect could be explained by variations in the diffusion of mobile receptors and/or the percentage of immobile ones. The diffusion of the mobile receptors was not signifi-

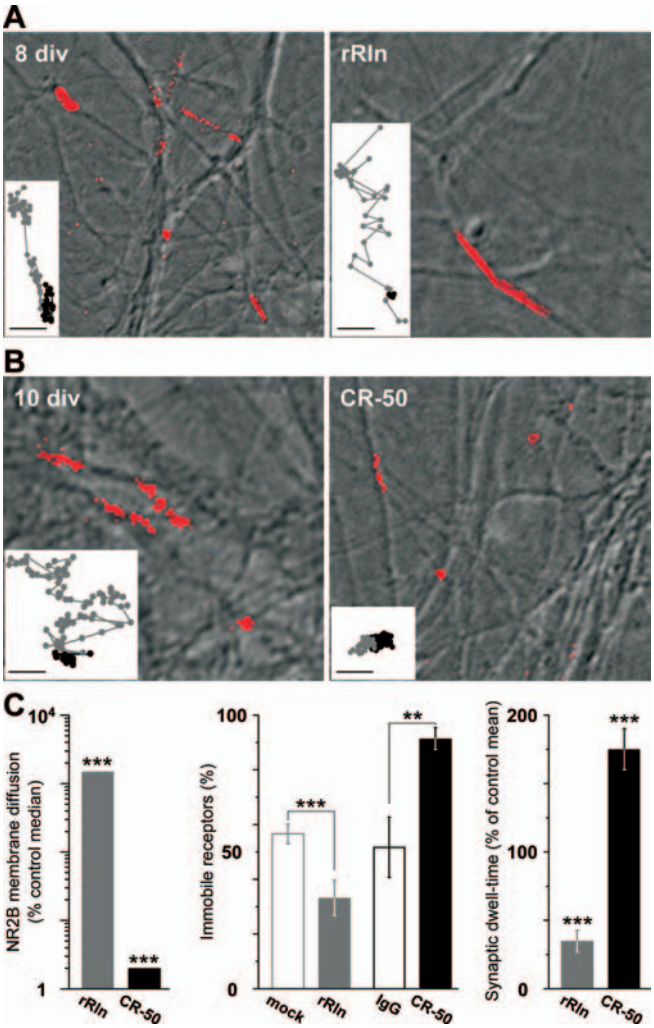

Figure 5. Reelin controls the surface mobility and synaptic residency time of 2B–NMDARs during maturation. ***A***, Representative summed trajectories of QDs coupled to NR2B subunits (red) at the surface of hippocampal neurons (differential interference contrast image) at 8 div either in control condition (mock; left) or after a chronic treatment with rRln (right). In control conditions, QD–NR2B display both diffusive (extended line) and immobile (dot-like) trajectories. Insets show examples of raw trajectories over 500–1000 frames in synaptic (black lines) and extrasynaptic compartments (gray lines; scale bars, 500 nm). ***B***, Same legend as ***A***, but examples of summed and raw trajectories were obtained in 10 div neurons either in control conditions (IgG) or after a chronic treatment with CR-50. ***C***, Left, Bar graph showing the synaptic instantaneous diffusion coefficients obtained at 8 div after treatment with rRln (1495%; $n = 58$; gray) and at 10–12 div after treatment with CR-50 (2%; $n = 68$; black). Values are expressed as the percentage change from age-matched median control value. Middle, Percentage of total immobile QD–NR2B obtained at 8 div either in control conditions (56.5 ± 3.6%; $n = 6$; open gray) or after treatment with rRln (33.1 ± 6.4%; $n = 6$; gray) and at 10–12 div in control conditions (51.6 ± 11.0%; $n = 5$; open black) or after treatment with CR-50 (91.3 ± 4.1%; $n = 5$; black). Single particles were considered immobile when the instantaneous diffusion coefficient was below 0.0075 $\mu m^2/s$. Right, Mean ± SEM of the synaptic residency time of exchanging QD–NR2B expressed as the percentage of age-matched control values. Note the significant decrease after treatment with rRln (34.9 ± 8.0%; $n = 58$) and increase after CR-50 antibody treatment (175 ± 15%; $n = 68$). $^{**}p \leq 0.01$; $^{***}p < 0.001$.

cantly different between control and rRln groups (control median of 0.14 $\mu m^2/s$; IQR of 0.07–0.25 $\mu m^2/s$, $n = 25$; rRln median of 0.15 $\mu m^2/s$, IQR of 0.1–0.26 $\mu m^2/s$, $n = 26$; $p = 0.47$), whereas rRln treatment decreased the percentage of immobile receptors (Fig. 5*C*, middle) ($p = 0.006$). These results indicate that rRln treatment increased the surface mobility of synaptic 2B–NMDARs by acting on receptor immobilization. We next examined the synaptic stability of these receptors by measuring the individual dwell time of receptors that exchange between the synaptic and extrasynaptic domains. In rRln-treated neurons, the 2B–NMDARs were on average present twofold less time within synapses compared with QD–NR2B in mock control conditions (Fig. 5*C*, right). However, the exchange frequency between the extrasynaptic and synaptic membrane remained unchanged (control, 0.92 ± 0.11 Hz, $n = 39$; rRln, 1.11 ± 0.13 Hz, $n = 42$; $p = 0.49$). These data ruled out the possibility that the rRln-induced decrease in synaptic retention of 2B–NMDARs resulted from a limited access of receptors to the postsynaptic membrane. Consistent with the observed decrease in ifenprodil sensitivity of NMDA–mEPSCs after chronic treatment with rRln (Fig. 1*A*), synaptic 2B–NMDARs are more diffusive and thus retained less within synapses when chronically exposed to rRln.

At synapses from 10–12 div neurons, endogenous Reelin decreased the number of functional NR1/NR2B receptors (Fig. 1). Strikingly, we found that CR-50 treatment significantly reduced both the surface explored (Fig. 5*B*) and the mobility (Fig. 5*C*) of synaptic 2B–NMDARs. This effect was concomitant with an increase in the percentage of immobile receptors (Fig. 5*C*, middle) ($p = 0.01$). Importantly, the time spent by the 2B–NMDARs in the synaptic compartment was significantly enhanced after CR-50 treatment (Fig. 5*C*, right). The increase in the synaptic dwell time was not accompanied by variation in the exchange frequency between extrasynaptic and synaptic membranes (control, 1.55 ± 0.12 Hz, $n = 44$; CR-50, 1.61 ± 0.31 Hz, $n = 24$; $p = 0.41$). These results indicate that blockade of Reelin function with CR-50 increased the retention of diffusing surface NR2B within synapses. Interestingly, blockade of the biosynthesis of Reelin with RlnAS mimicked the effect of CR-50 on the NR2B surface mobility. Indeed, in 10–12 div neurons, the surface mobility of synaptic 2B–NMDARs was significantly reduced by chronic treatment with the RlnAS (control median of 7.10^{-3} $\mu m^2/s$, IQR of 4.10^{-4}-3.10^{-2} $\mu m^2/s$, $n = 416$; RlnAS median of 4.10^{-3} $\mu m^2/s$, IQR of 8.10^{-6}-1.10^{-2} $\mu m^2/s$, $n = 177$; $p = 0.0019$). In addition, the synaptic dwell time was significantly increased (control, 0.2 ± 0.02 s, $n = 162$; RlnAS, 0.9 ± 0.24 s, $n = 66$; $p = 6.10^{-5}$). Thus, inhibition of Reelin function had opposite effects on the surface diffusion of native synaptic 2B–NMDARs compared with addition of rRln, that is a reduction of surface mobility and an increase of the time spent in the synaptic compartment.

Altogether, these data showed that the Reelin-dependent changes in the subunit composition of synaptic NMDARs were paralleled by profound effects on the surface mobility and residency time of synaptic 2B–NMDARs.

Role of β1-class integrins in the surface diffusion of native NR2B subunits

We examined whether chronic blockade of the function of the Reelin receptors of the β1-class integrins mimicked the effect of neutralizing the function of Reelin. Chronic treatment with the function-blocking antibody against the β1 subunit integrins decreased the surface diffusion of synaptic 2B–NMDARs in 10–12 div neurons (median of 12.10^{-3} $\mu m^2/s$, IQR of 7.10^{-4}-2.10^{-2} $\mu m^2/s$, $n = 53$) compared with age-matched IgM-treated neurons (median of 30.10^{-3} $\mu m^2/s$, IQR of 3.10^{-3}-0.11 $\mu m^2/s$, $n = 87$; $p = 0.02$). Thus, the recovery of functional synaptic 2B–NMDARs in neurons treated with the anti-β1 integrin function-blocking antibody was paralleled by a decrease in 2B–NMDAR surface mobility. In contrast to what was observed after neutralizing the function of Reelin, the dwell time of synaptic 2B–NMDARs was not affected by chronic blockade of the function of

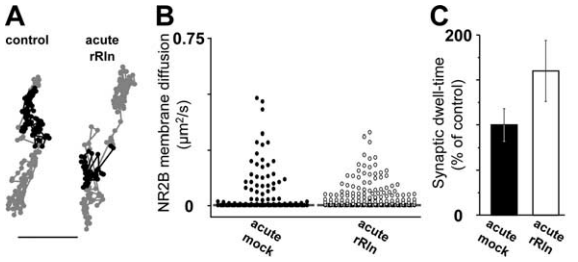

Figure 6. Acute treatment with recombinant Reelin does not affect 2B–NMDAR surface mobility. ***A***, Representative raw trajectories over 500–1000 frames of QD–NR2B in synaptic (black lines) and extrasynaptic (gray lines; scale bar, 500 nm) compartments at the surface of neurons after 15 min incubation with either the mock control (left) or rRln (right). ***B***, Vertical scatter plot distributions of the instantaneous diffusion coefficients of membrane 2B–NMDARs in acute mock (control; $n = 156$; black circles) and acute rRln ($n = 216$; open black) conditions. Each diffusion coefficient value is represented by a dot. The gray bar in each group represents the median value. ***C***, Synaptic residency time of exchanging QD–NR2B after acute incubation with either rRln (open black) or mock (black) expressed as the percentage of control value ($p > 0.05$).

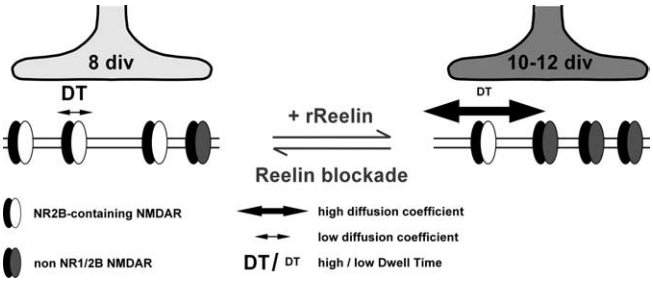

Figure 7. Schematic model of Reelin-dependent control of synaptic NMDAR maturation. Synaptic maturation between 8 and 10–12 div involves a loss of highly ifenprodil-sensitive NMDARs and an accumulation of Reelin at active synapses (dark gray). Addition of rRln to early synapses accelerated maturational processes, i.e., the loss of synaptic NR1/NR2B receptors. This was accompanied by changes in dwell time and diffusion coefficient of 2B–NMDARs. Blocking Reelin function at later stages (i.e., 10–12 div) had opposite effects, resulting in the recovery of synaptic NR1/NR2B receptors and a simultaneous decrease of their synaptic dwell time and an increase of their diffusion coefficient.

β1-class integrins (control IgM, 2.5 ± 0.36 s; anti-β1, 2.1 ± 0.28 s; $p > 0.05$). However, the percentage of 2B–NMDARs exchanging between synaptic and extrasynaptic membranes was significantly decreased (control IgM, 39 ± 5%; anti-β1, 21 ± 3%; $p < 0.05$). Altogether, these results indicate that the treatment with the anti-β1 antibody decreased the surface mobility of 2B–NMDARs by acting on the number of receptors exchanging between the extrasynaptic and synaptic compartments. Thus, chronic blockade of the function of the β1-class integrins mimicked the effect of neutralizing the function of Reelin on 2B–NMDARs synaptic surface trafficking but likely involved different mechanisms for the synaptic retention of 2B–NMDARs.

Reelin-induced changes in 2B–NMDAR surface mobility requires long-term treatment

To determine whether a chronic exposure (24 h) to rRln was necessary to induce changes in 2B–NMDAR surface trafficking, we measured the surface mobility of 2B–NMDARs during acute application (1–20 min) of an equivalent concentration of rRln (2.50–5.55 nM). As shown by the trajectories in Figure 6*A*, we found that acute rRln exposure did not change the surface diffusion of 2B–NMDARs. Quantitatively, there were no significant changes in the surface mobility (control median of 2.10^{-3} $\mu m^2/s$, IQR of 1.10^{-4}-2.10^{-2} $\mu m^2/s$, $n = 156$; acute rRln median of 4.10^{-3} $\mu m^2/s$, IQR of 2.10^{-4}-4.10^{-2} $\mu m^2/s$, $n = 216$; $p = 0.47$) or in the synaptic dwell time (control, 0.34 ± 0.06 s, $n = 136$; acute rRln, 0.57 ± 0.13 s, $n = 81$; $p = 0.09$) of QD–NR2B (Fig. 6*B*,*C*). Thus, a chronic exposure to rRln is required to modify surface 2B–NMDAR trafficking, consistent with the time course of changes in NMDAR subunit composition (Fig. 1) and Reelin expression during postnatal development (Sinagra et al., 2005).

Differential effect of Reelin on the surface mobility of native 2B–NMDARs and 2A–NMDARs

The electrophysiological results above clearly indicate that Reelin did not affect synaptic AMPAR currents but the question remains for NMDARs containing other subunits, such as NR2A. We tested whether the effects of Reelin were specific for 2B–NMDARs. Recent results showed that 2A–NMDARs and 2B–NMDARs are not exclusively segregated into synaptic or extrasynaptic compartments in cultured hippocampal neurons (Groc et al., 2006b; Thomas et al., 2006); thus, we compared the surface diffusion of synaptic and extrasynaptic 2B–NMDARs and 2A–NMDARs after chronic treatments with rRln or RlnAS. Addition of rRln induced in 8 div neurons a massive 15-fold increase of the synaptic 2B–NMDAR surface mobility (Fig. 5*C*) as well as a smaller but significant 1.7-fold increase in the membrane diffusion of synaptic 2A–NMDARs ($p = 0.021$; control, $n = 29$; rRln, $n = 23$). As illustrated by the reconstructed 2B–QD trajectories (Fig. 5*A*), the same treatment significantly increased the surface mobility of extrasynaptic 2B–NMDARs (control median of 6.10^{-3} $\mu m^2/s$, IQR of 0–7.10^{-2} $\mu m^2/s$, $n = 261$; rRln median of 8.10^{-2} $\mu m^2/s$, IQR of $1.5.10^{-3}$-24.10^{-2} $\mu m^2/s$, $n = 237$; $p \leq 0.0001$). In contrast, rRln had no significant effect on the surface mobility of extrasynaptic 2A–NMDARs in 8 div neurons (control median of 2.10^{-3} $\mu m^2/s$, IQR of 2.10^{-4}-13.10^{-2} $\mu m^2/s$, $n = 58$; rRln median of 2.10^{-3} $\mu m^2/s$, IQR of 1.10^{-4}-26.10^{-2} $\mu m^2/s$, $n = 45$; $p = 0.36$). In 10 div neurons chronically treated with RlnAS, the surface mobility of extrasynaptic 2B–NMDARs was significantly decreased (control median of 7.10^{-3} $\mu m^2/s$, IQR of 7.10^{-4}-3.10^{-2} $\mu m^2/s$, $n = 424$; RlnAS median of 3.10^{-4} $\mu m^2/s$, IQR of 7.10^{-6}-1.10^{-2} $\mu m^2/s$, $n = 358$; $p \leq 0.0001$) (see also 2B–QD trajectories in Fig. 5*B*). However, chronic treatment with RlnAS had no significant effect on the surface mobility of extrasynaptic 2A–NMDARs (control median of 1.10^{-4} $\mu m^2/s$, IQR of 5.10^{-6}-4.10^{-3} $\mu m^2/s$, $n = 78$; RlnAS median of 2.10^{-4} $\mu m^2/s$, IQR of 1.10^{-5}-3.10^{-3} $\mu m^2/s$, $n = 42$; $p = 0.32$). These results show that Reelin controls the surface mobility of 2B–NMDARs but not of 2A–NMDARs in the extrasynaptic compartment.

Discussion

Synaptic maturation is a dynamic process that continues long after synaptogenesis and enables synapses to stabilize their presynaptic and postsynaptic properties. In the present study, we provide evidences for a key role of the ECM protein Reelin in the control of synaptic NMDAR subunit composition during postnatal maturation of glutamatergic central synapses (Fig. 7). We have shown that blockade of the function of Reelin prevented the maturation-dependent reduction in 2B–NMDAR-mediated synaptic currents, whereas addition of recombinant Reelin during early stages of maturation dramatically accelerated the loss of NR1/NR2B receptor participation to NMDA-mediated synaptic currents. When we examined the cellular mechanisms involved in this process, we revealed that Reelin bidirectionally regulates the surface diffusion and synaptic residency time of 2B–NMDARs. Thus, we propose a developmental model in which changes in the Reelin concentration at the synapse regulate syn-

aptic NMDAR signaling and surface trafficking during maturation *in vitro* (Fig. 7).

At most newly formed glutamatergic synapses, NMDARs consist primarily of NR1/NR2B subunits, whereas NR2A are incorporated later in more mature synapses (van Zundert et al., 2004). Numerous studies revealed that the change in NMDAR subunit composition is critical for synaptic maturation, plasticity, and neuronal network refinement in different brain areas (Bear, 2003; Collingridge et al., 2004). NMDARs of the NR1/NR2B subtype can be distinguished from other subtypes of NMDARs based on their high sensitivity toward ifenprodil (Williams, 1993; Hatton and Paoletti, 2005). In the present report, we used ifenprodil at selective concentrations to block NR1/NR2B receptors (Kew et al., 1998; Tovar and Westbrook, 1999) to examine the participation of these receptors in NMDAR-mediated synaptic currents. The proportion of NMDA–mEPSCs blocked by ifenprodil was reduced during maturation, indicating a decrease in the contribution of NR1/NR2B receptors to synaptic responses. It should be noted that, in 10–12 div neurons, NMDA-mEPSCs were insensitive to low concentrations of ifenprodil, showing that 10–12 div synapses are devoid of NR1/NR2B diheteromers. Thus, Reelin levels regulate the presence of highly ifenprodil-sensitive NR1/NR2B NMDARs at the synapse.

We reported previously that the recovery of functional synaptic NR1/NR2B NMDARs after blockade of Reelin function was paralleled by a return of NR2B at synaptotagmin I-labeled synapses (Chavis, 2005), consistent with a redistribution of synaptic NR2B subunits. Here, we confirmed this result and showed that Reelin controls the surface distribution of 2B–NMDARs on neurites. Changes in Reelin levels affected specifically 2B–NMDAR surface trafficking in the extrasynaptic membrane, whereas changes in both 2A–NMDARs and 2B–NMDARs were observed in the synaptic membrane. In contrast to what was observed on synaptic 2B–NMDAR diffusion, Reelin only slightly affected the surface mobility of synaptic 2A–NMDARs. It is not clear whether the changes in synaptic 2A–NMDAR mobility reflect effects on synaptic NR1/NR2A diheteromers and/or on NR1/NR2B/NR2A triheteromers (Sheng et al., 1994; Tovar and Westbrook, 1999; Groc et al., 2006b; Thomas et al., 2006). However, the absence of an optical approach to specifically track triheteromers NR1/NR2B/NR2A (Groc et al., 2006b) and the lack of a specific NR2A subunit antagonist (Neyton and Paoletti, 2006) prevents the resolution of this issue.

The ECM protein regulates normal migration and positioning of neurons during embryonic development of laminated structures (Tissir and Goffinet, 2003). Despite the critical role of Reelin in embryonic brain development, the functional significance of the continued presence of Reelin in the normal postnatal brain remains unknown. Recent studies have shown the involvement of Reelin in hippocampal long-term potentiation, associative memory formation, dendritic growth, and modulation of glutamate-induced NMDAR activity, indicating the importance of Reelin in postnatal brain functions (Dityatev et al., 2006). Here, we provide evidence that Reelin is present at synaptic sites in dissociated cultures, consistent with immunohistochemical studies that have localized Reelin at dendritic spines (Pappas et al., 2001), associated with integrin receptors (Rodriguez et al., 2000) or intra-axonally (Derer et al., 2001; Martinez-Cerdeno et al., 2003; Ramos-Moreno et al., 2006). Most postnatal effects of Reelin reported so far are mediated by lipoprotein receptors (Niu et al., 2004; Beffert et al., 2005; Sinagra et al., 2005; Qiu et al., 2006; Qiu and Weeber, 2007). We reported previously that Reelin controls the somatic maturation of NMDARs through ApoER2/VLDLR (Sinagra et al., 2005). Interestingly, we report here that chronic blockade of ligand binding to all low-density lipoprotein receptor family members did not mimic the effect of blocking Reelin function. This finding not only eliminates the involvement of Reelin–lipoprotein receptor-mediated signaling but, more generally, it rules out the involvement of lipoprotein receptors in the maturation-dependent switch in synaptic NR2 subunits. Cell adhesion molecules of the β1-class integrins, namely $\alpha3\beta1$, have also been recognized as receptors for Reelin (Dulabon et al., 2000; Schmid et al., 2005). We found that maturation-dependent loss of synaptic NR1/NR2B receptors was blocked by chronic inhibition of β1-class integrins. Consistent with these data, the integrin subunit $\beta1$ has been localized by electron microscopy to dendritic spines in hippocampal neurons (Schuster et al., 2001). Moreover, pharmacological and genetic studies have implicated β1-class integrins in the regulation of synaptic functions and plasticity (Chun et al., 2001; Kramar et al., 2002; Chan et al., 2006; Huang et al., 2006). Thus, these data and our previous work (Sinagra et al., 2005) show that Reelin governs maturation of NMDARs in both somatic and synaptic compartments but involves different families of receptors.

Ionotropic glutamate receptors can traffic through different pathways in and from the synapses using both endocytotic/exocytotic and lateral diffusion processes (Groc and Choquet, 2006). Although NMDAR cycling is a key process to regulate the number of surface receptors (Wenthold et al., 2003), we did not observe Reelin-mediated changes in the surface expression of 2A–NMDARs and 2B–NMDARs. These results do not favor a regulation of synaptic 2B–NMDAR content by Reelin through cycling-dependent process. We showed previously that NMDAR surface mobility depends on their subunit composition because the surface mobility of 2A–NMDARs is smaller than that of 2B–NMDARs (Groc et al., 2006b). We proposed a new developmental model in which synaptic NMDARs subtypes are regulated by changes in surface trafficking during hippocampal maturation *in vitro* (Groc et al., 2006b). The present results not only strengthen but extent this model because Reelin-dependent changes in the NR2 subunit composition of synaptic NMDARs were paralleled by changes in 2B–NMDAR surface trafficking and synaptic stability. By which mechanism could Reelin regulate the synaptic residency time of 2B–NMDARs? Although this question remains fully open, a potential mechanism could involve changes in the levels and/or relocalization of scaffolding proteins, such as synapse-associated protein 102 and the postsynaptic density 95 (Sans et al., 2000).

During development, experience and neuronal activity affect the maturation of synaptic NMDARs, leading to the proposal that neuronal activity controls NMDAR subunit composition and the developmental NR2 subunit switch (Carmignoto and Vicini, 1992; Heynen et al., 2000; Hoffmann et al., 2000; Philpot et al., 2001), as well as the amplitude of AMPA–mEPSCs (Turrigiano et al., 1998). Here, we observed that the loss in ifenprodil sensitivity of 10–12 div neurons was not perturbed by chronic blockade of neuronal activity. Notably, we reported previously that, between 9 and 15 div, the changes in surface mobility of 2B–NMDARs were independent of global neuronal activity (Groc et al., 2006b). Finally, the mechanisms underlying the release of Reelin are independent of neural activity (Fig. 3), but rather they involve a constitutive pathway (Lacor et al., 2000). Thus, our results are consistent with a model in which Reelin is released in a neuronal activity-independent manner, and it is concentrated in maturing synapses in which it controls synaptic

NMDAR subunit composition by acting on surface trafficking of 2B–NMDARs (Fig. 7).

In conclusion, the results presented here reveal not only a central role of Reelin at postnatal excitatory synapses but also a new mode of control of synaptic NMDAR assembly and a new role of ECM proteins in regulating glutamate receptor surface diffusion. We propose that Reelin participates in the physiological maturation and plasticity properties of glutamate synapses. Thus, defects in the function of Reelin could participate in the development of abnormal glutamatergic transmission, which is thought to play a predominant role in neuropsychiatric disorders such as schizophrenia (Mohn et al., 1999; Tsai and Coyle, 2002; Fatemi, 2005).

References

Adesnik H, Nicoll RA, England PM (2005) Photoinactivation of native AMPA receptors reveals their real-time trafficking. Neuron 48:977–985.

Ashby MC, De La Rue SA, Ralph GS, Uney J, Collingridge GL, Henley JM (2004) Removal of AMPA receptors (AMPARs) from synapses is preceded by transient endocytosis of extrasynaptic AMPARs. J Neurosci 24:5172–5176.

Bear MF (2003) Bidirectional synaptic plasticity: from theory to reality. Philos Trans R Soc Lond B Biol Sci 358:649–655.

Beffert U, Weeber EJ, Durudas A, Qiu S, Masiulis I, Sweatt JD, Li WP, Adelmann G, Frotscher M, Hammer RE, Herz J (2005) Modulation of synaptic plasticity and memory by Reelin involves differential splicing of the lipoprotein receptor Apoer2. Neuron 47:567–579.

Borgdorff AJ, Choquet D (2002) Regulation of AMPA receptor lateral movements. Nature 417:649–653.

Carmignoto G, Vicini S (1992) Activity-dependent decrease in NMDA receptor responses during development of the visual cortex. Science 258:1007–1011.

Chan CS, Weeber EJ, Zong L, Fuchs E, Sweatt JD, Davis RL (2006) β1-integrins are required for hippocampal AMPA receptor-dependent synaptic transmission, synaptic plasticity, and working memory. J Neurosci 26:223–232.

Chavis P (2005) Reelin controls NMDA receptor subunit composition at hippocampal synapses during maturation. Soc Neurosci Abstr 31:730.9.

Chavis P, Westbrook G (2001) Integrins mediate functional pre- and postsynaptic maturation at a hippocampal synapse. Nature 411:317–321.

Chavis P, Mollard P, Bockaert J, Manzoni O (1998) Visualization of cyclic AMP-regulated presynaptic activity at cerebellar granule cells. Neuron 20:773–781.

Chun D, Gall CM, Bi X, Lynch G (2001) Evidence that integrins contribute to multiple stages in the consolidation of long term potentiation in rat hippocampus. Neuroscience 105:815–829.

Collingridge GL, Isaac JT, Wang YT (2004) Receptor trafficking and synaptic plasticity. Nat Rev Neurosci 5:952–962.

D'Arcangelo G, Curran T (1998) Reeler: new tales on an old mutant mouse. BioEssays 20:235–244.

D'Arcangelo G, Homayouni R, Keshvara L, Rice DS, Sheldon M, Curran T (1999) Reelin is a ligand for lipoprotein receptors. Neuron 24:471–479.

Derer P, Derer M, Goffinet A (2001) Axonal secretion of Reelin by Cajal-Retzius cells: evidence from comparison of normal and Reln(Orl) mutant mice. J Comp Neurol 440:136–143.

Dityatev A, Schachner M (2003) Extracellular matrix molecules and synaptic plasticity. Nat Rev Neurosci 4:456–468.

Dityatev A, Frischknecht R, Seidenbecher CI (2006) Extracellular matrix and synaptic functions. Results Probl Cell Differ 43:69–97.

Dulabon L, Olson EC, Taglienti MG, Eisenhuth S, McGrath B, Walsh CA, Kreidberg JA, Anton ES (2000) Reelin binds alpha3beta1 integrin and inhibits neuronal migration. Neuron 27:33–44.

Fatemi SH (2005) Reelin glycoprotein in autism and schizophrenia. Int Rev Neurobiol 71:179–187.

Flint AC, Maisch US, Weishaupt JH, Kriegstein AR, Monyer H (1997) NR2A subunit expression shortens NMDA receptor synaptic currents in developing neocortex. J Neurosci 17:2469–2476.

Garner CC, Zhai RG, Gundelfinger ED, Ziv NE (2002) Molecular mechanisms of CNS synaptogenesis. Trends Neurosci 25:243–251.

Groc L, Choquet D (2006) AMPA and NMDA glutamate receptor trafficking: multiple roads for reaching and leaving the synapse. Cell Tissue Res 326:423–438.

Groc L, Heine M, Cognet L, Brickley K, Stephenson FA, Lounis B, Choquet D (2004) Differential activity-dependent regulation of the lateral mobilities of AMPA and NMDA receptors. Nat Neurosci 7:695–696.

Groc L, Gustafsson B, Hanse E (2006a) AMPA signalling in nascent glutamatergic synapses: there and not there! Trends Neurosci 29:132–139.

Groc L, Heine M, Cousins SL, Stephenson FA, Lounis B, Cognet L, Choquet D (2006b) NMDA receptor surface mobility depends on NR2A–2B subunits. Proc Natl Acad Sci USA 103:18769–18774.

Hatton CJ, Paoletti P (2005) Modulation of triheteromeric NMDA receptors by N-terminal domain ligands. Neuron 46:261–274.

Herz J, Goldstein JL, Strickland DK, Ho YK, Brown MS (1991) 39-kDa protein modulates binding of ligands to low density lipoprotein receptor-related protein/alpha 2-macroglobulin receptor. J Biol Chem 266:21232–21238.

Heynen AJ, Quinlan EM, Bae DC, Bear MF (2000) Bidirectional, activity-dependent regulation of glutamate receptors in the adult hippocampus in vivo. Neuron 28:527–536.

Hiesberger T, Trommsdorff M, Howell BW, Goffinet A, Mumby MC, Cooper JA, Herz J (1999) Direct binding of Reelin to VLDL receptor and ApoE receptor 2 induces tyrosine phosphorylation of disabled-1 and modulates tau phosphorylation. Neuron 24:481–489.

Hoffmann H, Gremme T, Hatt H, Gottmann K (2000) Synaptic activity-dependent developmental regulation of NMDA receptor subunit expression in cultured neocortical neurons. J Neurochem 75:1590–1599.

Huang Z, Shimazu K, Woo NH, Zang K, Muller U, Lu B, Reichardt LF (2006) Distinct roles of the β1-class integrins at the developing and the mature hippocampal excitatory synapse. J Neurosci 26:11208–11219.

Kew JN, Richards JG, Mutel V, Kemp JA (1998) Developmental changes in NMDA receptor glycine affinity and ifenprodil sensitivity reveal three distinct populations of NMDA receptors in individual rat cortical neurons. J Neurosci 18:1935–1943.

Kirson ED, Yaari Y (1996) Synaptic NMDA receptors in developing mouse hippocampal neurones: functional properties and sensitivity to ifenprodil. J Physiol (Lond) 497:437–455.

Kramar EA, Bernard JA, Gall CM, Lynch G (2002) Alpha3 integrin receptors contribute to the consolidation of long-term potentiation. Neuroscience 110:29–39.

Lacor PN, Grayson DR, Auta J, Sugaya I, Costa E, Guidotti A (2000) Reelin secretion from glutamatergic neurons in culture is independent from neurotransmitter regulation. Proc Natl Acad Sci USA 97:3556–3561.

Lavezzari G, McCallum J, Dewey CM, Roche KW (2004) Subunit-specific regulation of NMDA receptor endocytosis. J Neurosci 24:6383–6391.

Li JH, Wang YH, Wolfe BB, Krueger KE, Corsi L, Stocca G, Vicini S (1998) Developmental changes in localization of NMDA receptor subunits in primary cultures of cortical neurons. Eur J Neurosci 10:1704–1715.

Martinez-Cerdeno V, Galazo MJ, Clasca F (2003) Reelin-immunoreactive neurons, axons, and neuropil in the adult ferret brain: evidence for axonal secretion of reelin in long axonal pathways. J Comp Neurol 463:92–116.

Miyata T, Nakajima K, Mikoshiba K, Ogawa M (1997) Regulation of Purkinje cell alignment by reelin as revealed with CR-50 antibody. J Neurosci 17:3599–3609.

Mohn AR, Gainetdinov RR, Caron MG, Koller BH (1999) Mice with reduced NMDA receptor expression display behaviors related to schizophrenia. Cell 98:427–436.

Monyer H, Burnashev N, Laurie DJ, Sakmann B, Seeburg PH (1994) Developmental and regional expression in the rat brain and functional properties of four NMDA receptors. Neuron 12:529–540.

Nakajima K, Mikoshiba K, Miyata T, Kudo C, Ogawa M (1997) Disruption of hippocampal development in vivo by CR-50 mAb against reelin. Proc Natl Acad Sci USA 94:8196–8201.

Neyton J, Paoletti P (2006) Relating NMDA receptor function to receptor subunit composition: limitations of the pharmacological approach. J Neurosci 26:1331–1333.

Niu S, Renfro A, Quattrocchi CC, Sheldon M, D'Arcangelo G (2004) Reelin promotes hippocampal dendrite development through the VLDLR/ApoER2-Dab1 pathway. Neuron 41:71–84.

Ogawa M, Miyata T, Nakajima K, Yagyu K, Seike M, Ikenaka K, Yamamoto H, Mikoshiba K (1995) The reeler gene-associated antigen on Cajal-Retzius neurons is a crucial molecule for laminar organization of cortical neurons. Neuron 14:899–912.

Pappas GD, Kriho V, Pesold C (2001) Reelin in the extracellular matrix and dendritic spines of the cortex and hippocampus: a comparison between wild type and heterozygous reeler mice by immunoelectron microscopy. J Neurocytol 30:413–425.

Perez-Otano I, Ehlers MD (2005) Homeostatic plasticity and NMDA receptor trafficking. Trends Neurosci 28:229–238.

Philpot BD, Sekhar AK, Shouval HZ, Bear MF (2001) Visual experience and deprivation bidirectionally modify the composition and function of NMDA receptors in visual cortex. Neuron 29:157–169.

Qiu S, Weeber EJ (2007) Reelin signaling facilitates maturation of CA1 glutamatergic synapses. J Neurophysiol 97:2312–2321.

Qiu S, Zhao LF, Korwek KM, Weeber EJ (2006) Differential reelin-induced enhancement of NMDA and AMPA receptor activity in the adult hippocampus. J Neurosci 26:12943–12955.

Ramos-Moreno T, Galazo MJ, Porrero C, Martinez-Cerdeno V, Clasca F (2006) Extracellular matrix molecules and synaptic plasticity: immunomapping of intracellular and secreted Reelin in the adult rat brain. Eur J Neurosci 23:401–422.

Roche KW, Standley S, McCallum J, Dune Ly C, Ehlers MD, Wenthold RJ (2001) Molecular determinants of NMDA receptor internalization. Nat Neurosci 4:794–802.

Rodriguez MA, Pesold C, Liu WS, Kriho V, Guidotti A, Pappas GD, Costa E (2000) Colocalization of integrin receptors and reelin in dendritic spine postsynaptic densities of adult nonhuman primate cortex. Proc Natl Acad Sci USA 97:3550–3555.

Sans N, Petralia RS, Wang YX, Blahos II J, Hell JW, Wenthold RJ (2000) A developmental change in NMDA receptor-associated proteins at hippocampal synapses. J Neurosci 20:1260–1271.

Schmid RS, Jo R, Shelton S, Kreidberg JA, Anton ES (2005) Reelin, integrin and DAB1 interactions during embryonic cerebral cortical development. Cereb Cortex 15:1632–1636.

Schuster T, Krug M, Stalder M, Hackel N, Gerardy-Schahn R, Schachner M (2001) Immunoelectron microscopic localization of the neural recognition molecules L1, NCAM, and its isoform NCAM180, the NCAM-associated polysialic acid, beta1 integrin and the extracellular matrix molecule tenascin-R in synapses of the adult rat hippocampus. J Neurobiol 49:142–158.

Sheng M, Cummings J, Roldan LA, Jan YN, Jan LY (1994) Changing subunit composition of heteromeric NMDA receptors during development of rat cortex. Nature 368:144–147.

Shi J, Aamodt SM, Constantine-Paton M (1997) Temporal correlations between functional and molecular changes in NMDA receptors and GABA neurotransmission in the superior colliculus. J Neurosci 17:6264–6276.

Sinagra M, Verrier D, Frankova D, Korwek KM, Blahos J, Weeber EJ, Manzoni OJ, Chavis P (2005) Reelin, very-low-density lipoprotein receptor, and apolipoprotein E receptor 2 control somatic NMDA receptor composition during hippocampal maturation *in vitro*. J Neurosci 25:6127–6136.

Stocca G, Vicini S (1998) Increased contribution of NR2A subunit to synaptic NMDA receptors in developing rat cortical neurons. J Physiol (Lond) 507:13–24.

Thomas CG, Miller AJ, Westbrook GL (2006) Synaptic and extrasynaptic NMDA receptor NR2 subunits in cultured hippocampal neurons. J Neurophysiol 95:1727–1734.

Tissir F, Goffinet AM (2003) Reelin and brain development. Nat Rev Neurosci 4:496–505.

Tovar KR, Westbrook GL (1999) The incorporation of NMDA receptors with a distinct subunit composition at nascent hippocampal synapses *in vitro*. J Neurosci 19:4180–4188.

Tovar KR, Westbrook GL (2002) Mobile NMDA receptors at hippocampal synapses. Neuron 34:255–264.

Tsai G, Coyle JT (2002) Glutamatergic mechanisms in schizophrenia. Annu Rev Pharmacol Toxicol 42:165–179.

Turrigiano GG, Leslie KR, Desai NS, Rutherford LC, Nelson SB (1998) Activity-dependent scaling of quantal amplitude in neocortical neurons. Nature 391:892–896.

van Zundert B, Yoshii A, Constantine-Paton M (2004) Receptor compartmentalization and trafficking at glutamate synapses: a developmental proposal. Trends Neurosci 27:428–437.

Wenthold RJ, Prybylowski K, Standley S, Sans N, Petralia RS (2003) Trafficking of NMDA receptors. Annu Rev Pharmacol Toxicol 43:335–358.

Williams K (1993) Ifenprodil discriminates subtypes of the *N*-methyl-D-aspartate receptor: selectivity and mechanisms at recombinant heteromeric receptors. Mol Pharm 44:851–859.